Journal of Energy Storage 49 (2022) 104173

Contents lists available at ScienceDirect

Journal of Energy Storage

journal homepage: www.elsevier.com/locate/est

Research Papers

Environmentally friendly high performance Zn-air rechargeable battery using cellulose derivatives: A 3D-printed prototype

Tibor Nagy [a], Lajos Nagy [a], Zoltán Erdélyi [b], Eszter Baradács [b,c], György Deák [a], Miklós Zsuga [a], Sándor Kéki [a,*]

[a] Department of Applied Chemistry, Faculty of Sciences and Technology, University of Debrecen, Egyetem tér 1, Debrecen H-4032, Hungary
[b] Department of Solid State Physics, Faculty of Sciences and Technology, University of Debrecen, P.O. Box 400, Debrecen H-4002, Hungary
[c] Department of Environmental Physics, Faculty of Sciences and Technology, University of Debrecen, Poroszlay u. 6, Debrecen H-4026, Hungary

ARTICLE INFO

Keywords:
Zn-air secondary battery
Cellulose derivatives
Environmentally friendly
Biodegradable
3D printing

ABSTRACT

In this paper an environmentally friendly high performance prototype of rechargeable Zn-air battery using cellulose based biodegradable matters as additive and diaphragm is reported. During designing we were aspired to construct a heavy metal free cell containing nontoxic, commercially available biodegradable feedstock. The fix cell geometry was granted by 3D-printing. Charging/discharging cycle tests were performed using cotton lattice or cellophane diaphragms separately. The presence of carboxymethyl cellulose sodium salt (CMC-Na, Mn: 90 kDa and 250 kDa with $f = 0.7$ or $f = 1.2$ average functionality) additives in the electrolyte was also tested. Significant difference was found between the cells operated with and without additives. Two main benefits of the application of CMC-Na salts were observed: (i) by increasing the viscosity of the electrolyte the rate of evaporization of the water was decreased; (ii) owing to the higher viscosity of the lye and the good chelating agent properties of the carboxyl functional groups more stable cell operation was obtained. Using cotton lattice as diaphragm, 100% Coulomb efficiency was detected during the entire measurement (more than 1000 cycles), while the weight of zinc electrode was constant and its surface remained smooth. Additional cyclic voltammetry tests were also carried out to investigate the electrode processes and the change of the electrode surface was monitored by scanning electron microscopy.

1. Introduction

In the last decades the use of green, renewable energy and thus, the storage and utilization of the energy have become one of the most important and developing research area in the energy sector. Owing to their high energy density (more than 1080 Wh/kg) nature and safely operation zinc-air batteries have attracted much attention as possible alternative solutions [1,2]. However, the morphology control of zinc deposition upon charging and ensuring appropriate catalyst(s) for the oxygen evolution/reduction reactions (OER/ORR) are the two main challenges concerning zinc-air cells. The inhibition of dendritic deposition promoted by modification of electrolyte [3] can be the cheapest and easiest way from the various available methods such as anode engineering, ion transfer control, electric field regulation, etc. Nevertheless, from the cathode point of view, construction of an environmental friendly zinc-air cell is a serious challenge. The reversibility of oxygen evolution/reduction reactions is essential for improving the performance of a zinc-air batteries. Furthermore, the adsorption of the oxygen on the different electro catalysts affects the type of the ORR reaction (direct four- and two-electron pathways) [4,5]. The applied catalysts can be monofunctional by catalyzing the OER [6,7] or the ORR [8–10] reactions, while the bifunctional catalyst can promote both reactions [11,12]. Among the developed catalysts, metal-based and metal-free can be distinguished. The metal-based ones usually contain heavy metal ions such as platinum, ruthenium, iridium, cobalt etc. [13–16]. The metal-free catalysts that can be alternatives for constructing environmental friendly cells, are usually modified carbon nanotubes and graphene [17–19], and though these carbon-based materials are widely used as a mechanically robust skeleton of both types of catalysts (metal-free and metal-based) [20,21]. Application of binders are necessary for the preparation of these type catalysts. However, degradation of the binder can take place during the operation of the cell, decreasing the lifetime of zinc-air battery [22], Therefore, to handle this problem, binder-free, self-supported catalysts were also developed [23,

* Corresponding author.
E-mail address: keki.sandor@science.unideb.hu (S. Kéki).

https://doi.org/10.1016/j.est.2022.104173
Received 6 September 2021; Received in revised form 22 January 2022; Accepted 4 February 2022
Available online 10 February 2022

24].

As it turns out from the literature background on zinc-air battery, the cells investigated consisted of one or more special components (heavy metals, e.g. Pt based catalysts) to ensure the sufficient performance. However, these components are very expensive and/or inaccessible on the market [25–27] and are not compatible with the aspirations of green development. Recently, we have reported a novel rechargeable zinc-air cell [28] using binder and heavy metal-free pure charcoal cathode obtaining good charging/discharging performance. The dendritic deposition on the surface of Zn anode was also minimized by applying dicarboxyl poly(ethylene glycol) additive in the electrolyte. As a continuation of our earlier works, in this paper, we focus our attention on designing a prototype of rechargeable Zn-air battery making it high performance operation and more environmental friendly. During designing we were aspired to construct a heavy metal free cell containing nontoxic, commercially available, cheap biodegradable feedstock.

In this new rechargeable Zn-air battery, the graphite/charcoal cathode was immersed into concentrated KOH solution saturated with $K_2[(Zn(OH)_4)]$ electrolyte containing high molecular weight carboxymethyl cellulose sodium salts (CMC-Na), as a commercially available chelating additive [29,30]. The charcoal owing to its adsorptive nature serves as a reservoir for the "*in situ*" evolved oxygen in the cathode during the OER reaction. The higher viscosity of the electrolyte by addition of CMC-Na can also aid keeping oxygen in the charcoal. In addition, the separator is a crucial part of the cell providing the appropriate ion conductivity and separation of the electrodes [31,32]. To develop and to simplify of our prototype cell, we used cellulose based, single layer separator for our environmental friendly zinc-air cell. Furthermore, to ensure the fix cell geometry, 3D-printer was used for printing polypropylene parts of the cell out.

2. Materials and methods

2.1. Materials

The graphite rod electrode with spectroscopic purity was purchased from Ceramics Praha (Czech Republic, Prague). Zinc foil (thickness 0.65 mm, Rheinzink, EN/DIN 988) was used. The zinc electrodes were rinsed with n-hexane then allowed to dry before use. n-Hexane (HPLC grade), Potassium hydroxide (analytical grade), Charcoal (analytical grade), Zinc oxide (analytical grade), were purchased from VWR (Debrecen, Hungary). The carboxymethyl cellulose Na salts (CMC—Na, $M_n = 90$ kDa and 250 kDa with different ($f = 0.7$ or $f = 1.2$) functionalities, respectively) and zinc wire (diameter: 0.5 mm, 99.99%) were obtained from Sigma-Aldrich. All chemicals were used as received.

2.2. Potentiostat

The cyclic charging discharging test of 3D-printed zinc-air rechargeable battery and the cyclic voltammetry (CV) measurements were performed by BioLogic SP-150 potentiostat (Seyssinet-Pariset, France) equipped with EC-Lab software package. The working potential range was chosen from 0.7 V to 1.9 V for the charging/discharging cycle tests with current density

2 $mAcm^{-2}$, while the voltammograms were recorded in the range of −0.5–0.55 V vs. cell potential with 20 mV/s scan rate.

2.3. Scanning electron microscopy (SEM)

The morphology of the surface of Zn electrode was visualized by Scanning Electron Microscopy (SEM) (Hitachi S-4300 scanning electron microscope (Tokyo, Japan)).

2.4. Viscosimetry

The viscosimetric measurements were carried out by a Master Smart viscometer produced by Fungilab S.A. (Barcelona, Spain), at the temperature of 25 °C.

2.5. Construction of Zn-air rechargeable batteries

The skeleton of Zn-air battery cells were designed by Tinkercad (Autodesk, Inc, online cloud platform) then all parts of the cell were printed out by Prusa i3 MK3S 3D printer using polypropylene (PP) filament (Fiberlogy). The applicability of the PP was tested by soaking it in lye (6 M KOH solution containing 0.25 M ZnO) for 24 h. Based on three parallel measurements no significant changes in the weight of the PP container were observed. Then two different orientations (horizontal and vertical) of the cells were planned and used for the measurements. The arrangements of the Zn-air rechargeable batteries are shown in Fig. 1 and Fig. 2. Cellophane or cotton (soaked in lye for 1 h before use) was used as diaphragm for the cell, the shape of the diaphragm was constructed for fitting into the inner space of the polypropylene (PP) skeleton. The zinc anode plate (cut from the zinc foil, length 10 cm, width 10 mm, thickness 0.65 mm) was fixed to the PP skeleton keeping constant distance (1.5 mm) between the zinc anode and the diaphragm. Then a mud was made from charcoal and 6 M aqueous potassium hydroxide solution containing ZnO and CMC-Na at a concentrations of 0.25 M and 2 m/v% (2 g CMC—Na was dissolved in 100 mL lye), respectively. The mud obtained was loaded into the PP skeleton interior space containing approximately 22 g charcoal. The filled PP skeleton was placed into the PP container in which the level of the lye was kept constant.

2.6. Air cathode

The air cathode was constructed from the charcoal and the graphite rod. The charcoal was soaked for 8 h in the electrolyte to obtain the mud before the use. No further additive and/or catalyst were used.

3. Results and discussion

The development of Zn–air rechargeable batteries is a widely investigated research area nowadays. However, most of the research concentrate on the general challenges of the Zn anode and the application of bifunctional catalyst systems [33]. Additionally, many studies are applying only half cells, thus the importance of membranes is not properly investigated yet. However, the membrane has very important role in the performance of Zn-air batteries, since the membrane can effectively regulate the ion transport between the anode and the cathode [34]. In our previous work, we have used a combination of cellophane and cotton cloth as a membrane and charcoal based air cathode in our novel Zn-air rechargeable battery. Herein, we investigated the applicability of both membranes separately.

First, the applicability of swollen cotton cloth in the Zn-air rechargeable battery was checked by charging-discharging tests and we found an excellent battery performance. Fig. 3. shows 1000 cycles of charging-discharging events. The working potential range is small, it is around 0.2 V (1.2V-1.4 V), and stable performance was observed during the whole 1000 cycles. At the beginning of the cycling test higher potential range was recorded, however, stable working potential range was achieved after some cycles.

The working potential seems to be low, compared to those reported in the literature, where 1.65 V equilibrium cell potential is typically accepted. However, in our prototype, the pure charcoal acts as a catalyst for oxygen evolution/reduction reactions (ORR/OER) by adsorbing the "*in situ*" formed O_2. Low redox potentials for O_2 reduction, even near zero under alkaline conditions have been reported for different types of carbon-based electro catalysts. The low potential value was explained by

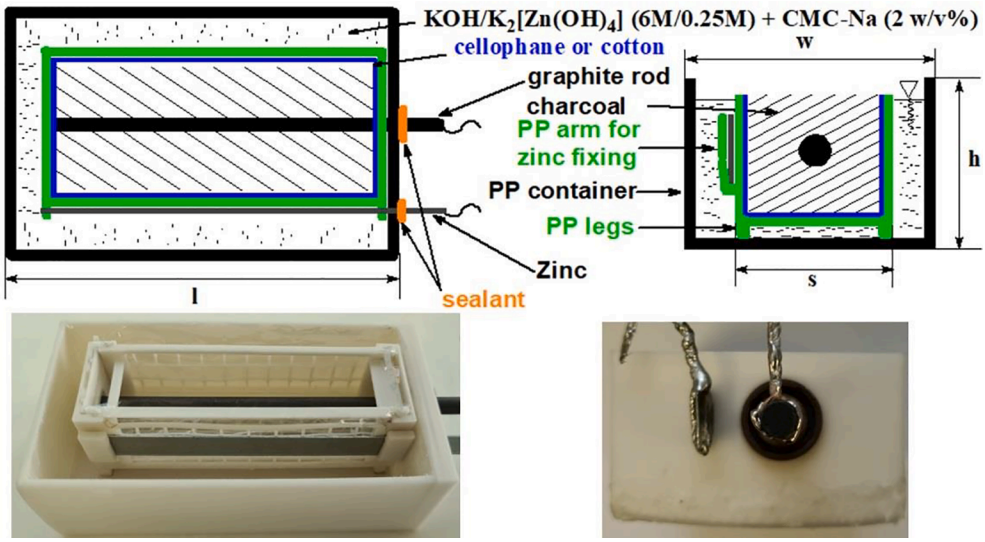

Fig. 1. Arrangements of the Zn-air rechargeable battery with horizontal orientation (dimensions $w = 65$ mm, $s = 30$ mm, $h = 42$ mm, $l = 129$ mm).

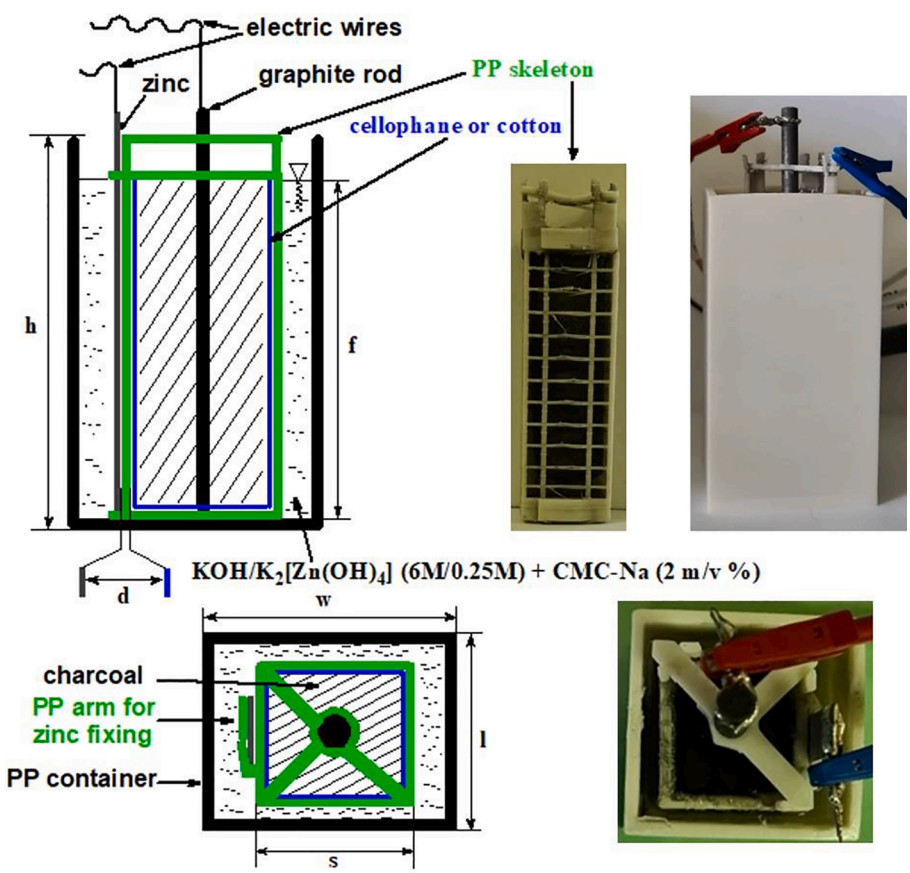

Fig. 2. Arrangements of the Zn-air rechargeable battery with vertical orientation (dimensions $w = 60$ mm, $s = 30$ mm, $h = 110$ mm, $d = 1.5$ mm, $l = 50$ mm, $f = 100$ mm).

the higher activity of edges serving as active sites for reduction of oxygen [35]. Furthermore, Qu and Yeager suggested the formation of peroxide ion pathway to explain the lower potentials obtained [36,37]. The gross electrochemical processes are shown in Scheme 1.

As it can be seen in Scheme 1, if the reduction of the oxygen takes place according to the 4 electron pathway, the well-known ~1.65 V equilibrium potential can be obtained for a zinc-air battery. However, it was also shown that using carbon based cathode the two electron pathway process (shown in Scheme 1) may become dominant [37]. In our particular case, the cell potential of our zinc-air battery was lower (~1.3 V) than 1.65 V. Based on this experimental finding we came to the conclusion that the two electron pathway as dominant process takes place in the cathode compartment. In this case, the equilibrium cell potential calculated from the standard electrode potentials is 1.195 V. Furthermore, it has been reported that the HO_2^- adsorbed on carbon is stable under alkaline conditions. Thus, during the investigated cycling

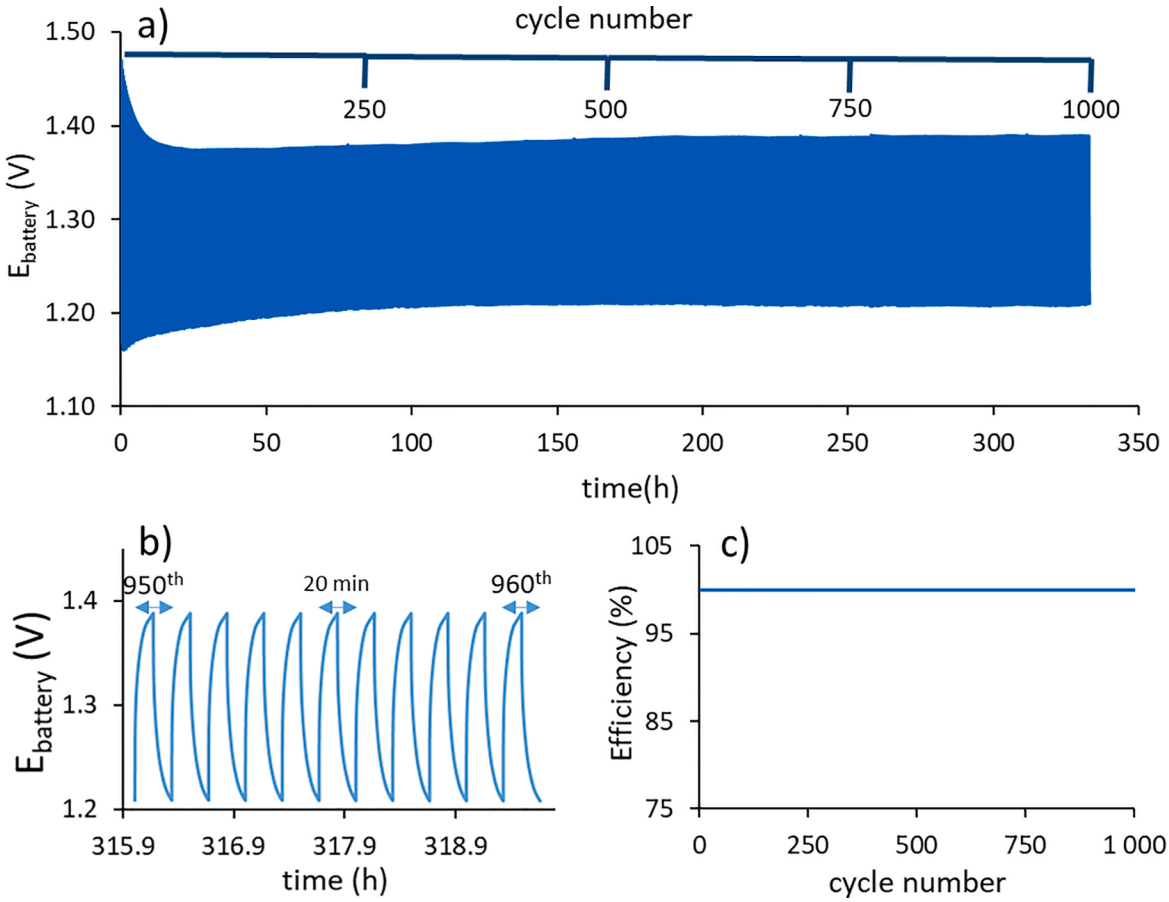

Fig. 3. The cycling test (a, b) and the Coulomb efficiency (c) of the 3D-printed rectangular Zn-air rechargeable battery, equipped with cotton cloth membrane. The current density was kept to be constant, i.e., 2 mAcm^{-2}, while the time limit of charging and discharging was set to 10 min.

time applied for the cycling test its significant decomposition should not take place in the absence of additional catalyst [37]. The stability and the negligible decomposition of HO_2^- was supported by the high reproducibility of cycling test (Fig. 3).

In order to investigate the electrochemical reactions, long-term charging of the battery was performed. A charging process is shown in the Supporting Information as Fig. S1.

The 1.65 V charging potential was achieved only after 61.1 h. We suggest that the low working potential (<1.4 V) is the result of the combination of different possible oxygen reduction pathways.

To suppress the undesirable dissolution of Zn anode yielding H_2 evolution via $[Zn(OH)_4]^{2-}$, we used concentrated KOH solution saturated with $K_2[Zn(OH)_4]$. It must be noted, that preliminary experiments were carried out to identify the cell potential where the formation of hydrogen is relevant. It was found that significant evolution of H_2 occurs only at charging potential higher than 2 V.

The Coulomb efficiency has been found to be 100% during the whole experiment. This finding shows an excellent balance between the charging and discharging cycles in the operating battery. No change in the mass of the Zn- electrode was found. Based on these results, the swollen cotton cloth membrane properly stabilized the ion transport hence, highly regulates the reactions on the surface of the Zn electrode. Such regulation is necessary to avoid the formation of an undesired metallic Zn dendrite formation on the surfaces the electrode.

With the parameters of 2 mAcm^{-2} charging current density and 10 min time frame, the capacity was found to be 2.63 mAh. It should be noted that similar current densities were applied in several Zn-Air battery studies [19,38–41].

The cycling test and the Coulomb efficiency of the 3D-printed rectangular Zn-air rechargeable battery equipped with cotton cloth membrane is shown in Fig. 3. The current density was kept constant at 2 mAcm^{-2}, while the time limit of charging and discharging was set to 10 min (1000 cycle).

On the other hand, in the case of cellophane (Fig. S2). the cell potential was within a low range and stable performance was obtained up to 500 charging-discharging cycle. Similarly to the swollen cotton cloth, at the beginning of the test higher potential range was observed. Since the cell with cotton cloth has higher physical resistance than that of the cellophane, only the cell prepared with cotton cloth was used for further experiments.

3.1. Gelation with CMC-Na salts

The most common electrolyte for the Zn-air batteries is KOH solution of different concentrations. However, there are two major problems associated with the presence of strong alkaline solutions. The first problem is the capturing of CO_2 from the air, resulting in the formation of undesirable precipitate giving rise to uncontrolled change in the composition of the electrolyte solution. The second major problem is the evaporation of water from the electrolyte

Many studies [40] used pure oxygen, however, these results cannot be adopted to air electrode systems. We created an open charcoal based cathode in which the "*in situ*" forming O_2 is captured by adsorption during the charging process. Thus, small amount of supplementary oxygen is freely entering the cathode giving rise to limited air transport and, hence, the formation of carbonates highly reduces.

The evaporation of water can be regulated by the viscosity of the electrolyte. The higher viscosity decreases the ion transport but usually decreases the efficiency of the secondary batteries [42]. Thus the selection of a proper viscosity modifier is important. In our rechargeable

Zn-air battery, carboxy methyl cellulose Na salts (CMC-Na) with different molecular weights and functionality have been applied.

To test the effect of the molecular weight of CMC—Na on battery performance, first CMC-Na salt was tested with lower molecular weight (90 kDa, 0.7 functionality). The cyclic performance test was carried out up to 400 cycles, as seen in Fig. 4.

After a short instacionary state, the potential range is decreasing, reaching a range of 0.3 V (1.05–1.35 V). This range is close to the one measured with the electrolyte in the absence of a viscosity modifier. In addition to the excellent cyclic performance, high Coulomb efficiency was also observed. Capacity was found to be the same as in the case of electrolyte containing CMC-Na (250 kDa, 1.2 functionality). In both experiments, the batteries were charged and discharged with the same current density without reaching the set potential limits. The performance of the cycling tests with the use of CMC—Na (250 kDa, $f = 1.2$) is shown in Fig. 5.

As seen in Fig. 5, applying CMC-Na (250 kDa, $f = 1.2$), the performance of the secondary battery is appropriate, since none of the cycles reaches the set potential limits (0.7 V and 1.9 V).

The Coulomb efficiency during the cycling test was constant (100%). On the contrary, CMC-Na salt with the same molecular weight but with lower functionality (0.7 *vs.* 1.2) resulted in poorer performance (Fig. S3 in supporting information). All the cycles reached the set potential limits within the applied time frame, and changing capacity was observed from cycle to cycle. Despite the lower performance, the Coulomb efficiency was still 100%, which suggests an appropriate charging-discharging balance.

In addition, the energy efficiencies were also calculated. The highest value was obtained in the case of the additive-free cells (91%). Applying additives CMC—Na 90 kDa, f:0.7, 250 kDa, f:1.2 and 250 kDa, f:0.7, 80%, 64% and 60% energy efficiencies were obtained, respectively. The energy efficiency versus cycle number plots are shown in the Supporting Information (Figs. S4–S7).

3.2. Mathematical modeling of discharging process

In order to model mathematically the potential change during the discharging process of a battery, the 200th cycle was selected in each case. Recently, we have shown that the stretched exponential function, supplemented by a fast decay component was successfully applicable to model the potential change during the discharging steps [28]. In general, the stretched exponential function is suitable for the mathematical modeling of different disordered systems such as electrochemical reactions with a broad activation energy distribution [43]. The following equation was fitted (Eq. (1)) to the 200th cycle of all the cycling performance tests.

$$E_{battery}(t) = \Delta E_f e^{-k_f t} + \Delta E_s e^{-(k_s t)^{\beta}} + E_{\infty} \quad (1)$$

where ΔE_f and ΔE_s are the potential change, k_f and k_s are the rate

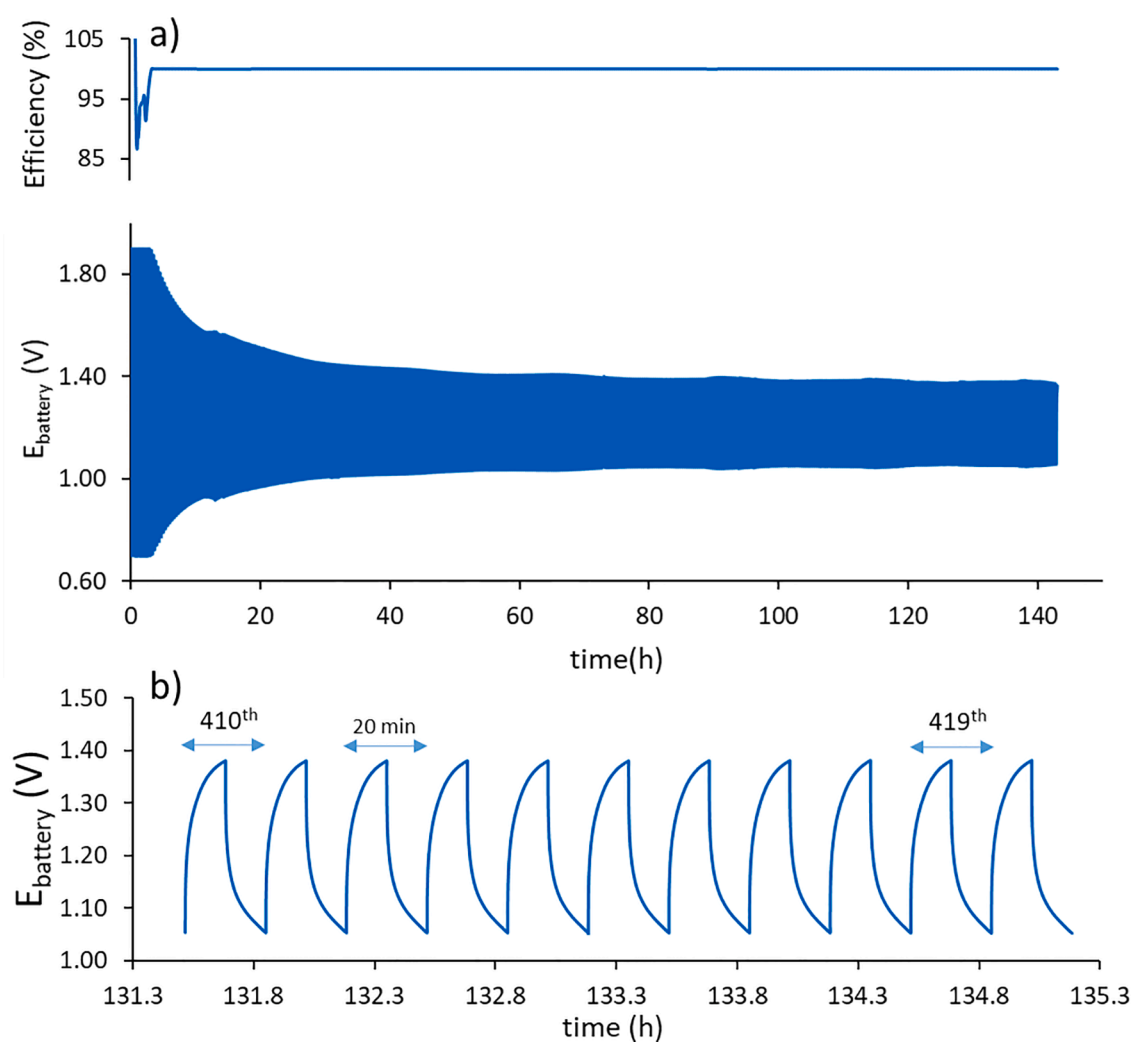

Fig. 4. Cycling test and Coulomb efficiency of 3D-printed Zn-air battery filled with KOH saturated with $K_2[Zn(OH)_4]$ electrolyte containing 2 m/v% CMC-Na (90 kDa with 0.7 functionality).

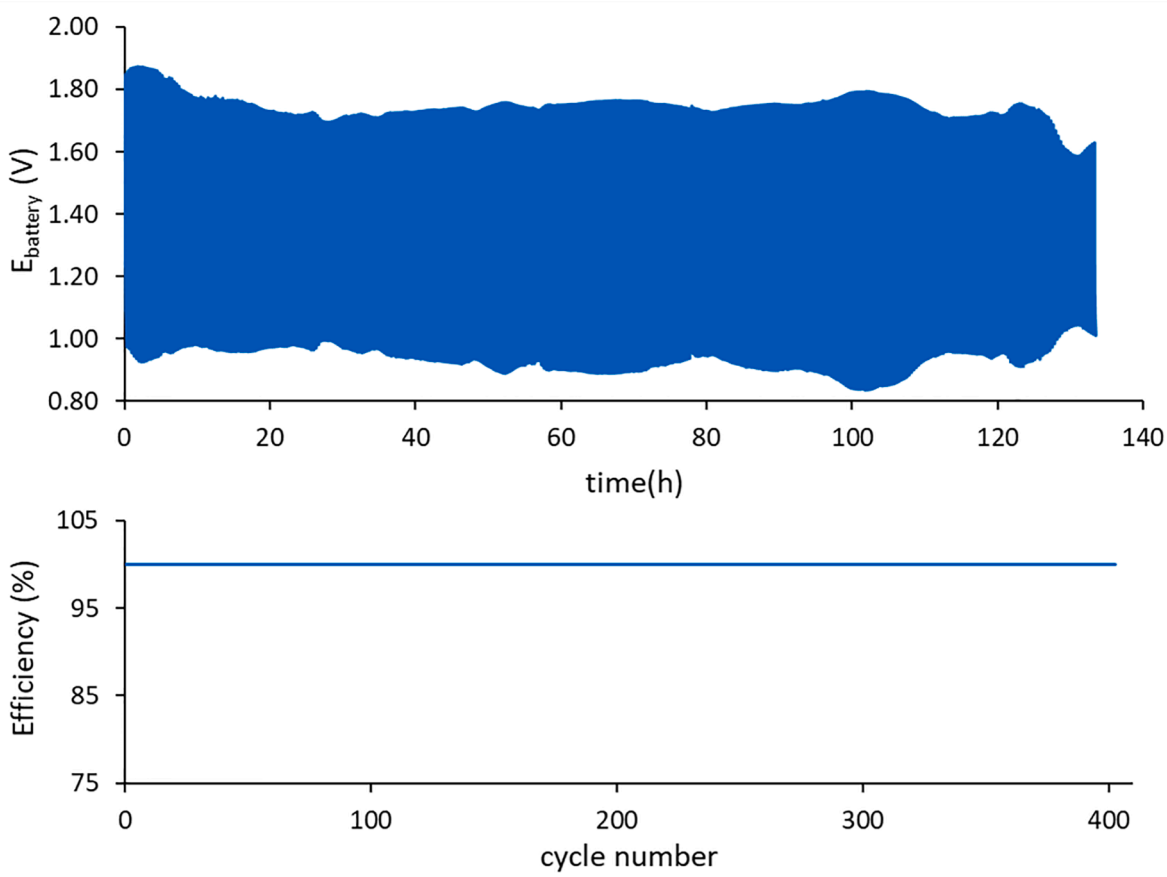

Fig. 5. Cycling test and the Coulomb efficiency of 3D-printed Zn air battery filled with KOH saturated with $K_2[Zn(OH)_4]$ electrolyte containing 2 m/v% CMC-Na (M_n=250 kDa, f = 1.2).

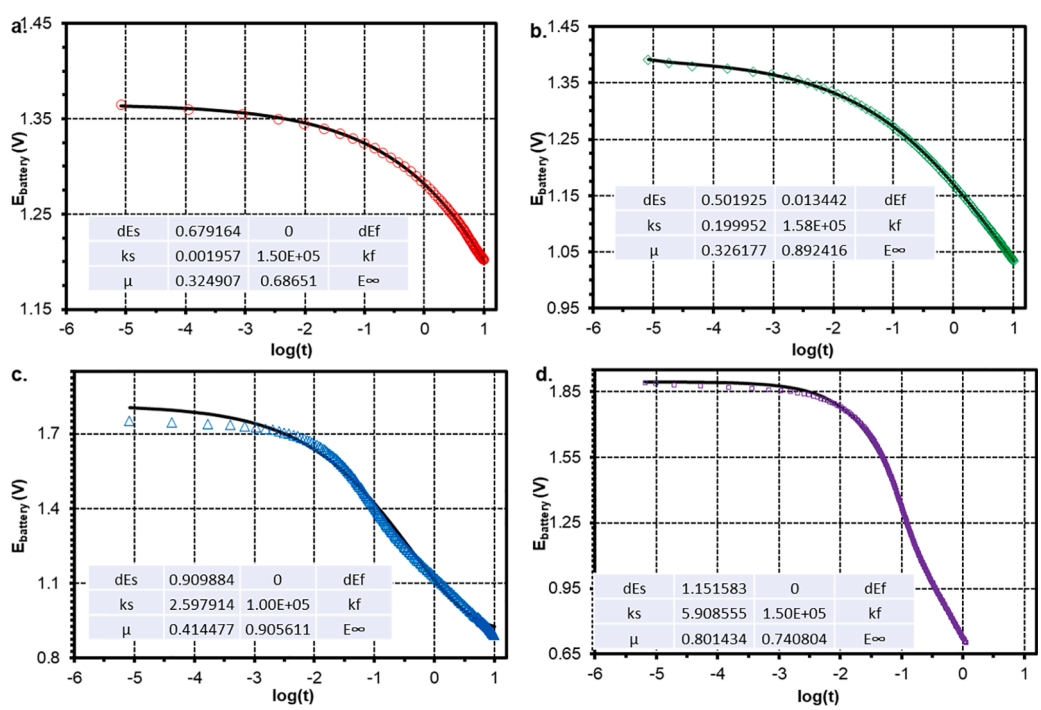

Fig. 6. Discharging (200th cycle) of the Zn-air rechargeable battery in the absence (a) and presence of CMC—Na viscosity modifiers, M_n=90 kDa, f = 0.7 (b), M_n=250 kDa, f = 1.2 (c), M_n=250 kDa, f = 0.7 (d) The black solid lines represent the fitted curves by Eq. (1) while the fitting parameters are shown in the tables.

coefficients of the fast and slow decay, respectively. The μ is the stretching exponent, while the E_∞ is the terminal potential.

In the case of additive-free electrolyte the stretched exponential function was applied, without the fast decay component of Eq. (1). As seen in Fig. 6., good agreements were found between the measured and fitted curves in each case. However, complex, two component decay was observed only with CMC—Na (90 kDa, f:0.7), where the ΔE_f and k_f were obtained to be 0.013 V and 158,000 min^{-1}, respectively. For other additives, CMC—Na 250 kDa, f:1.2 and f:0.7, the fast decay term was not necessary to be involved in the model. Similar stretching exponents were found for the additive-free and CMC—Na (90 kDa, $f = 0.7$) systems (0.32). The stretching exponent increases with the molecular weight of the CMC—Na. The highest value was determined for the CMC—Na (250 kDa, $f = 0.7$).

3.3. Cyclic voltammetry

For the investigation of anode reactions, i.e., zinc deposition and dissolution, further cyclic voltammetry measurements were carried out. The reference electrode was a zinc wire, and the voltammograms were recorded in the range of −0.5–0.55 V vs. cell potential. The voltammograms obtained in the presence and in the absence of CMC—Na salts are shown in Fig. 7.

All the cyclic voltammograms show clear oxidation and reduction peaks. Characteristic data obtained from the cyclic voltammetry measurements are summarized in Table 1.

Without any viscosity modifier, both anodic and cathodic peak positions are around 0.061 V and −0.128 V with peak separations approximately 0.2 V. Applying CMC—Na salts, higher anodic and cathodic shifts were recognized as compared to the additive-free electrolyte. It was found that the anodic peak shift was the highest for the CMC—Na with M_n=250 kDa and $f = 0.7$ functionality, while in the case of other two CMC—Na salts similar anodic shifts were observed. The cathodic shifts are higher than the anodic ones but their values are very similar. By applying the shifts, the peak separation can be calculated. Low separation is preferable since usually, it means low over potential. Low separations were found in the case of additive-free electrolyte (0.189 V). In the presence of CMC—Na additives in the electrolyte higher peak separation were obtained. The CMC—Na additives with M_n=250 kDa ($f = 1.2$) and 90 kDa ($f = 0.7$) have similar values, while the CMC—Na with M_n=250 kDa ($f = 0.7$) resulted in higher separation (0.3 V). The peak separations are likely depend on the viscosity of the solution and the functionality of the applied CMC—Na. The dynamic viscosity of the CMC-Na salt-containing electrolytes are 7.5, 48 and 75 Pas for the M_n=90 kDa ($f = 0.7$), M_n=250 kDa ($f = 0.7$) and M_n=250 kDa ($f = 1.2$) additives, respectively. In spite of the fact that there is one order of magnitude difference in the viscosities, similar peak separation was found for the CMC—Na additives with M_n=250 kDa ($f = 1.2$) and M_n=90 kDa ($f = 0.7$). This finding reflects the double functions of the additives i.e., altering the rate of the electrochemical reactions on the surface of the Zn electrode through the control of ion mobility by the electrolyte viscosity and formation of stable chelate complex with Zn^{2+} ions. These findings are in line with the cycling tests of the batteries with different viscosity modifiers. The profiles of the cyclic voltammograms at low voltages i.e., at around −0.5 V vs. cell potential can be ascribed to the electrochemical processes accompanied by the corrosion of Zn electrode.

In order to investigate the low charging potentials, additional CV measurement was carried out applying the charcoal-based cathode in the presence of additives (CMC—Na, 250 kDa ($f = 1.2$) The parameters all were the same as those used for the other CV measurements. The obtained cyclic voltammogram is shown in Fig. 8.

The cyclic voltammogram is similar to those presented in Fig. 7. Accordingly, clear oxidation and reduction peaks are observed indicating the presence of electrochemical reactions, i.e., the charcoal cathode does not act as a (super)capacitor.

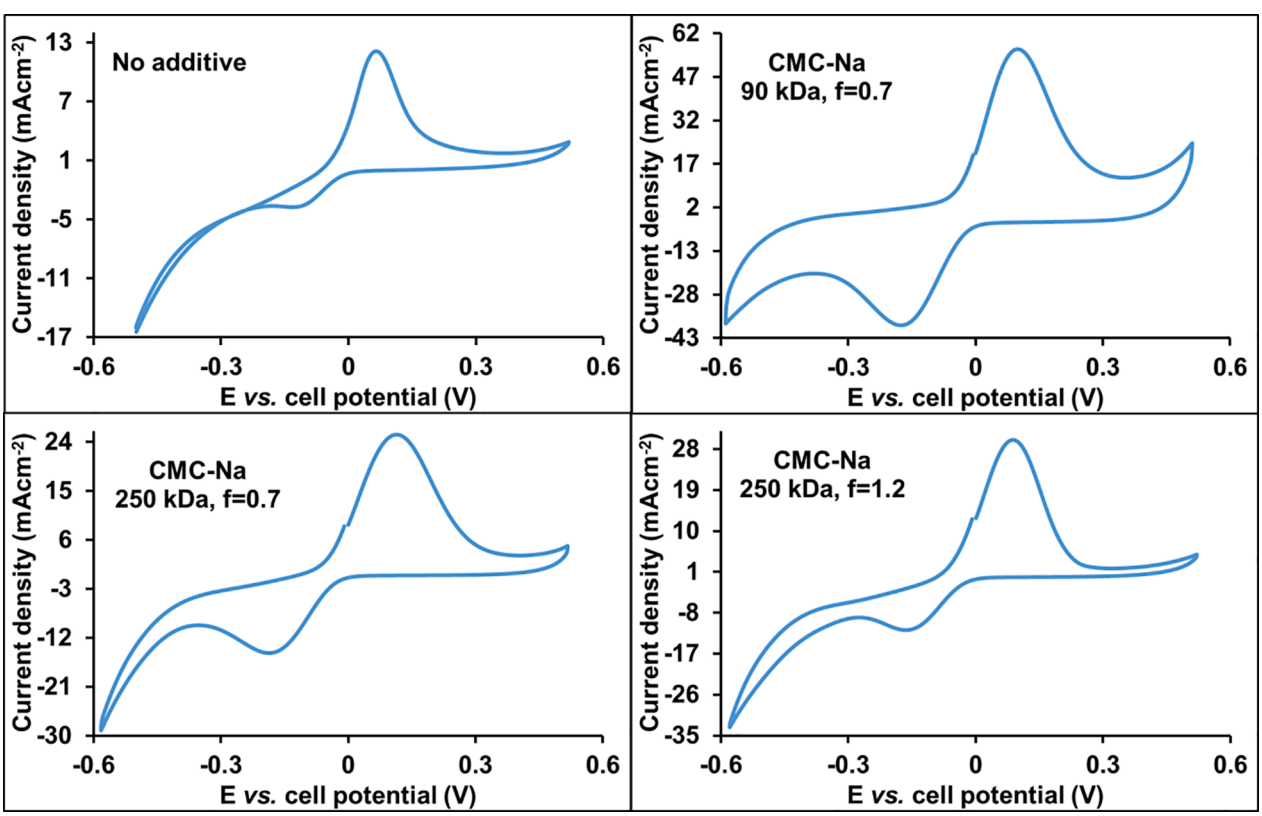

Fig. 7. Cyclic voltammograms obtained in the absence and in the presence of CMC-Na additives.

Table 1
The results of cyclic voltammetry including the electrolyte densities, the positions of anodic/cathodic peaks, the current densities and the peaks separations.

Additive	Viscosity of electrolyte(mPas)	Anodic peak position(E vs cell potential)	Cathodic peak position(E vs cell potential)	Anodic/Cathodic peakseparation	Anodic current density(mAcm^{-2})	Cathodic current density(mAcm^{-2})
no additive	1.5	0.061 V	−0.128 V	0.189 V	27.3	9.1
90 kDa, (f = 0.7)	7.5	0.096 V	−0.177 V	0.273 V	20.5	13.5
250 kDa, (f = 0.7	48	0.114 V	−0.188 V	0.302 V	9.7	5.7
250 kDa, (f = 1.2)	75	0.088 V	−0.164 V	0.252 V	10.7	4.4

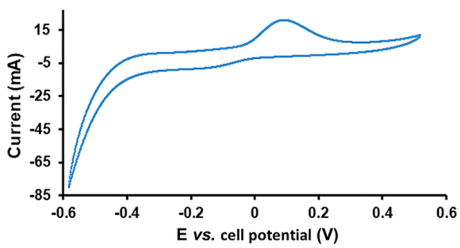

Fig. 8. The cyclic voltammogram obtained from the test of our Zn-air rechargeable battery prototype.

3.4. Scanning electron microscopy

Visually, the formation of deposits was not observed. In order to get deeper knowledge on the morphology change of the surface of Zn electrode, scanning electron microscopy measurements were carried out. After completing the experiments, the electrodes were washed with water and acetone then stored in cyclohexane prior to analysis.

The SEM images confirm the results of visual analysis, i.e., the lack of formation of deposits on the surface of the electrodes (Fig. 9). The morphology of the electrode surface changed differently in the absence and in the presence of CMC-Na additives, mossy-like deposition was formed without additive (after 1000 charging-discharging cycles). Applying the CMC-Na as viscosity modifier, dendrite and mossy depositions were significantly suppressed.

Additionally, the elemental analysis was performed by energy dispersive spectroscopy for all electrodes, where in addition to zinc, titanium, copper potassium carbon and oxygen have been found. EDS spectra are shown in the supporting information (Figs. S8–S12). The titanium and the copper are the alloying elements of the zinc (standard EN/DIN 988) while the potassium originated from the alkaline solution.

4. Conclusion

A rechargeable Zn-air alkaline battery was created applying 3D-printing and utilizing biodegradable and commercially available materials. The swollen cotton cloth proved to be a suitable cell membrane. High regulation on the ion transfer resulting in the significant suppression of dendrite and mossy formation and stable long-term battery performance were attained over 1000 charging-discharging cycles. The Coulomb efficiency was determined to be 100%, and no change in the mass of the Zn anode before and after use was found. It is to be noted that H_2 evolution was not observed during the cyclic performance tests. We have successfully applied carboxymethyl cellulose sodium salts

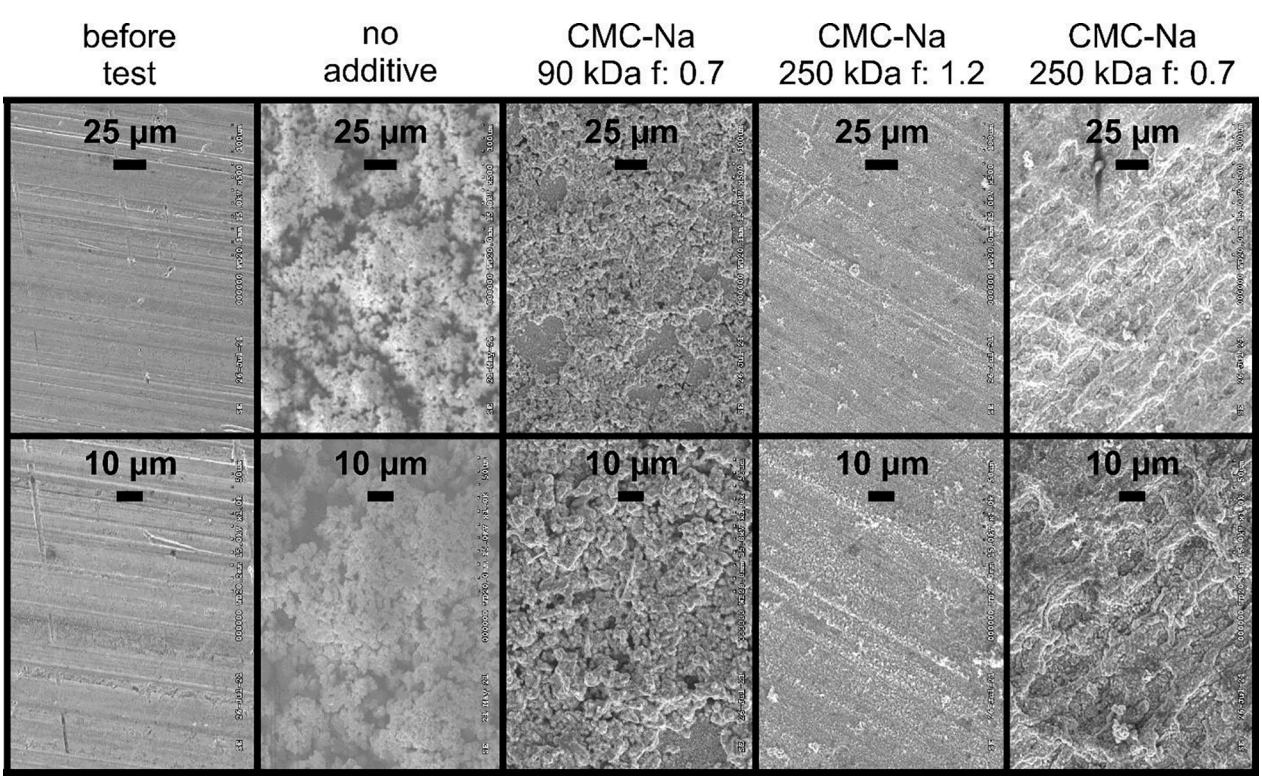

Fig. 9. The SEM images of the zinc electrode, obtained with the battery equipped by cotton cloth diaphragm in the absence and presence of CMC-Na additives (the electrodes were obtained from cyclic performance tests presented in Fig. 7.).

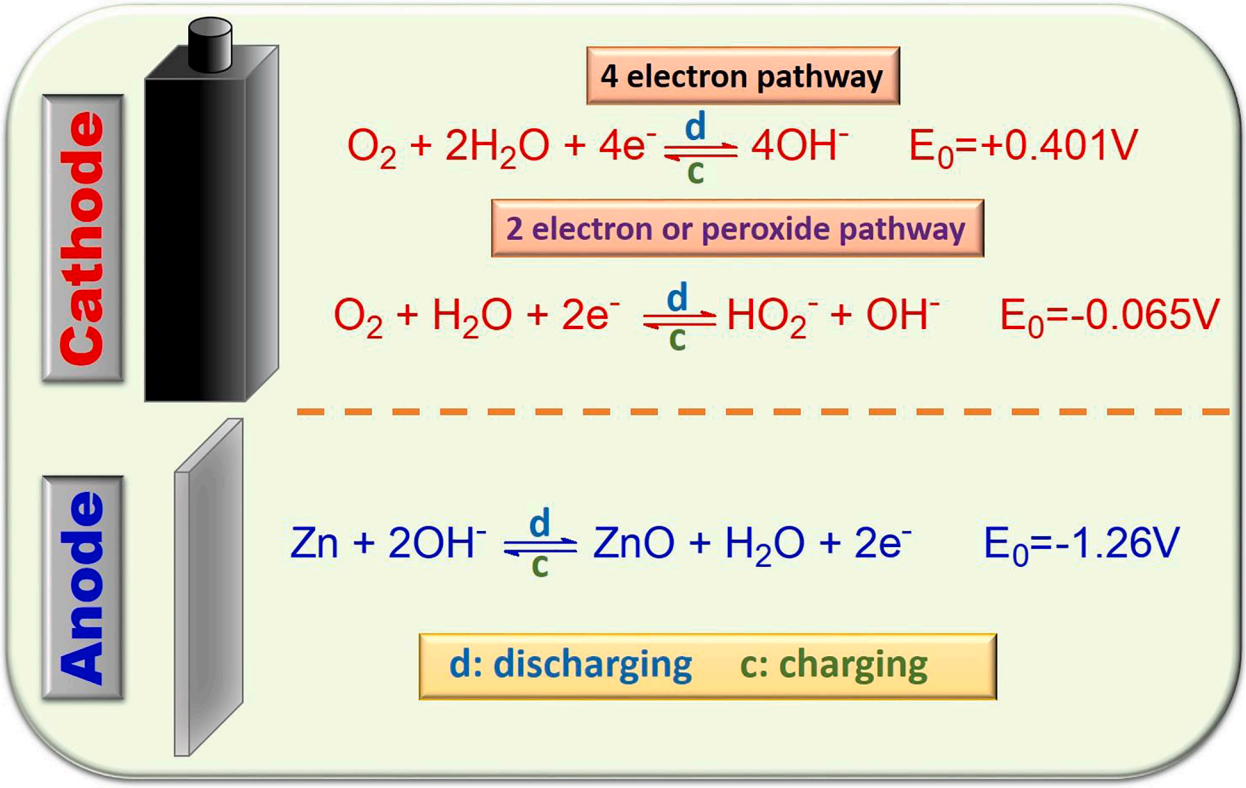

Scheme 1. The gross electrochemical processes of a Zn–air battery.

(CMC-Na) with different molecular weights and functionality to solve the general problem of water loss and to control the ion mobility in the electrolyte. However, the CMC-Na salts were found to have double functions: (i) increase the viscosity of the electrolyte thus decreasing the rates of evaporation of water and (ii) control the electrochemical reactions to form stable complex with the Zn^{2+} ions minimizing the zinc deposit formation. Based on these results, the lower viscosity of electrolyte and higher functionality of CMC-Na salts may be more preferable for a high-performance battery.

To investigate the Zn electrode reactions cyclic voltammetry measurements were carried out. Higher peak separation was observed for the CMC-Na containing electrolytes than for the additive-free one as it was expected based on their higher viscosities.

The discharging steps of the 200th cycle of all electrolyte systems were modeled mathematically by a stretched exponential function. Excellent agreement was found between the measured and calculated values. Applying the CMC-Na (90 kDa, $f = 0.7$) complex discharge process was identified since a fast decay component was necessary to implement into the model. The obtained stretching exponent was found to increase with the increasing molecular weight of CMC-Na additive, while a lower functionality resulted in a further increase. All our findings have been supported by scanning electron microscopy measurements showing that smooth electrode surface was obtained after long-term performance tests.

CRediT authorship contribution statement

Tibor Nagy: Conceptualization, Methodology, Writing – original draft. **Lajos Nagy:** Conceptualization, Methodology, Writing – original draft. **Zoltán Erdélyi:** Methodology. **Eszter Baradács:** Methodology. **György Deák:** Methodology. **Miklós Zsuga:** Conceptualization, Methodology, Writing – original draft, Writing – review & editing, Supervision. **Sándor Kéki:** Conceptualization, Writing – review & editing, Supervision.

Declaration of Competing Interest

The authors declare that they have no known competing financial interests or personal relationships that could have appeared to influence the work reported in this paper.

Acknowledgement

The work was supported by the Thematic Excellence Program (TKP2020-NKA-04) of the Ministry for Innovation and Technology in Hungary.

Supplementary materials

Supplementary material associated with this article can be found, in the online version, at doi:10.1016/j.est.2022.104173.

References

[1] M. Armand, J.M. Tarascon, Building better batteries, Nature 451 (2008) 652–657, https://doi.org/10.1038/451652a.
[2] J.S. Lee, S.T. Kim, R. Cao, N.S. Choi, M. Liu, K.T. Lee, J. Cho, Metal-air batteries with high energy density: Li-air versus Zn-Air, Adv. Energ. Mater. 1 (2010) 34–50, https://doi.org/10.1002/aenm.201000010.
[3] M. Kim, D. Yun, J. Jeon, Effect of a bromine complex agent on electrochemical performances of zinc electrodeposition and electrodissolution in Zinc-Bromide flow battery, J. Power Sources 438 (2019), 227020, https://doi.org/10.1016/j.jpowsour.2019.227020.
[4] Y. Guo, Y.N. Chen, H. Cui, Z. Zhou, Bifunctional electrocatalysts for rechargeable Zn-air batteries, Chin. J. Catal. 40 (2019) 1298–1310, https://doi.org/10.1016/S1872-2067(19)63349-8.
[5] W. Fang, J. Zhao, W. Zhang, P. Chen, Z. Bai, M. Wu, Recent progress and future perspectives of flexible Zn-air batteries, J. Alloy. Compd. 869 (2021), 158918, https://doi.org/10.1016/j.jallcom.2021.158918.
[6] J.E. Park, M.S. Lim, J.K. Kim, H.J. Choi, Y.E. Sung, Y.H. Cho, Optimization of cell components and operating conditions in primary and rechargeable zinc-air battery, J. Ind. Eng. Chem. 69 (2019) 161–170, https://doi.org/10.1016/j.jiec.2018.09.023.

[7] J.S. Lee, G. Nam, J. Sun, S. Higashi, H.W. Lee, S. Lee, W. Chen, Y. Cui, J. Cho, Composites of a prussian blue analogue and gelatin-derived nitrogen-doped carbon-supported porous spinel oxides as electrocatalysts for a Zn-air battery, Adv. Energy Mater. 6 (2016), 1601052, https://doi.org/10.1002/aenm.201601052.
[8] I.E.L. Stephens, A.S. Bondarenko, U. Grønbjerg, J. Rossmeisl, I. Chorkendorff, Understanding the electrocatalysis of oxygen reduction on platinum and its alloys, Energy Environ. Sci. 5 (2012) 6744–6762, https://doi.org/10.1039/C2EE03590A.
[9] C. Wang, N.M. Markovic, V.R. Stamenkovic, Advanced platinum alloy electrocatalysts for the oxygen reduction reaction, ACS Catal. 2 (2012) 891–898, https://doi.org/10.1021/cs3000792.
[10] T. Yu, D.Y. Kim, H. Zhang, Y. Xia, Platinum concave nanocubes with high-index facets and their enhanced activity for oxygen reduction reaction, Angew. Chem. Int. Ed. 50 (2011) 2773–2777, https://doi.org/10.1002/anie.201007859.
[11] C. Tang, Q. Zhang, Nanocarbon for oxygen reduction electrocatalysis: dopants, edges, and defects, Adv. Mater. 29 (2017), 1604103, https://doi.org/10.1002/adma.201604103.
[12] S. Clark, A. Latz, B. Horstmann, Rational development of neutral aqueous electrolytes for Zinc-air batteries, ChemSusChem 10 (2017) 4735–4747, https://doi.org/10.1002/cssc.201701468.
[13] Z.F. Huang, J. Wang, Y. Peng, C.Y. Jung, A. Fisher, X. Wang, Design of efficient bifunctional oxygen reduction/evolution electrocatalyst: recent advances and perspectives, Adv. Energy Mater. 7 (2017), 1700544, https://doi.org/10.1002/aenm.201700544.
[14] Y. Jiang, Y.P. Deng, J. Fu, D.U. Lee, R. Liang, Z.P. Cano, Y. Liu, Z. Bai, S. Hwang, L. Yang, D. Su, W. Chu, Z. Chen, Interpenetrating triphase cobalt-based nanocomposites as efficient bifunctional oxygen electrocatalysts for long-lasting rechargeable Zn-air batteries, Adv. Energy Mater. 8 (2018), 1702900, https://doi.org/10.1002/aenm.201702900.
[15] Y. Wei, M. Wang, N. Xu, L. Peng, J. Mao, Q. Gong, J. Qiao, Alkaline exchange polymer membrane electrolyte for high performance of all-solid-state electrochemical devices, ACS Appl. Mater. Interfaces 10 (2018) 29593–29598, https://doi.org/10.1021/acsami.8b09545.
[16] A.K. Worku, D.W. Ayele, N.G. Habtu, Recent advances and future perspectives in engineering of bifunctional electrocatalysts for rechargeable zinc-air batteries, Mater. Today Adv. 9 (2021), 100116, https://doi.org/10.1016/j.mtadv.2020.100116.
[17] L. Liu, X. Zhang, F. Yan, B. Geng, C. Zhu, Y. Chen, Self-supported N-doped CNT arrays for flexible Zn-air batteries, J. Mater. Chem. A 8 (2020) 18162–18172, https://doi.org/10.1039/D0TA05510G.
[18] L. Poolnapol, W. Kao-ian, A. Somwangthanaroj, F. Mahlendorf, M.T. Nguyen, T. Yonezawa, S. Kheawhom, Silver decorated reduced graphene oxide as electrocatalyst for Zinc-air batteries, Energies 13 (2020) 462–475, https://doi.org/10.3390/en13020462.
[19] H.B. Yang, J. Miao, S.F. Hung, J. Chen, H.B. Tao, X. Wang, L. Zhang, R. Chen, J. Gao, H.M. Chen, L. Dai, B. Liu, Identification of catalytic sites for oxygen reduction and oxygen evolution in N-doped graphene materials: development of highly efficient metal-free bifunctional electrocatalyst, Sci. Adv. 2 (2016), e1501122, https://doi.org/10.1126/sciadv.1501122.
[20] C. Zhu, Y. Aoki, H. Habazaki, Co 9 S 8 Nanoparticles incorporated in hierarchically porous 3D few-layer graphene-like carbon with S,N-doping as superior electrocatalyst for oxygen reduction reaction, Part. Part. Syst. Charact. 34 (2017), 1700296, https://doi.org/10.1002/ppsc.201700296.
[21] Y.J. Wang, H. Fan, A. Ignaszak, L. Zhang, S. Shao, D.P. Wilkinson, J. Zhang, Compositing doped-carbon with metals, non-metals, metal oxides, metal nitrides and other materials to form bifunctional electrocatalysts to enhance metal-air battery oxygen reduction and evolution reactions, Chem. Eng. J. 348 (2018) 416–437, https://doi.org/10.1016/j.cej.2018.04.208.
[22] Y. Fan, S. Ida, A. Staykov, T. Akbay, H. Hagiwara, J. Matsuda, K. Kaneko, T. Ishihara, Ni-Fe nitride nanoplates on nitrogen-doped graphene as a synergistic catalyst for reversible oxygen evolution reaction and rechargeable Zn-air battery, Small 13 (2017), 1700099, https://doi.org/10.1002/smll.201700099.
[23] N. Xu, J.A. Wilson, Y.D. Wang, T. Su, Y. Wei, J. Qiao, X.D. Zhou, Y. Zhang, S. Sun, Flexible self-supported bi-metal electrode as a highly stable carbon- and binder-free cathode for large-scale solid-state zinc-air batteries, Appl. Catal. B Environ. 272 (2020), 118953, https://doi.org/10.1016/j.apcatb.2020.118953.
[24] N. Radenahmad, R. Khezri, A.A. Mohamad, M.T. Nguyen, T. Yonezawa, A. Somwangthanaroj, S. Kheawhom, A durable rechargeable zinc-air battery via self-supported MnOx-S air electrode, J. Alloy. Compd. 883 (2021), 160935, https://doi.org/10.1016/j.jallcom.2021.160935.
[25] H.W. Kim, J.M. Lim, H.J. Lee, S.W. Eom, Y.T. Hong, S.Y. Lee, Artificially engineered, bicontinuous anion-conducting/-repelling polymeric phases as a selective ion transport channel for rechargeable zinc-air battery separator membranes, J. Mater. Chem. A 4 (2016) 3711–3720, https://doi.org/10.1039/C5TA09576J.
[26] A. Münchinger, K.D. Kreuer, Selective ion transport through hydrated cation and anion exchange membranes I. The effect of specific interactions, J. Membr. Sci. 592 (2019), 117372, https://doi.org/10.1016/j.memsci.2019.117372.
[27] Z. Yuan, H. Zhang, X. Li, Ion conducting membranes for aqueous flow battery systems, Chem. Commun. 54 (2018) 7570–7588, https://doi.org/10.1039/C8CC03058H.
[28] T. Nagy, L. Nagy, Z. Erdélyi, E. Baradács Gy. Deák, M. Zsuga, S. Kéki, Environmentally friendly Zn-air rechargeable battery with heavy metal free charcoal based air cathode, Electrochim. Acta 368 (2021), 137592, https://doi.org/10.1016/j.electacta.2020.137592.
[29] J. Liu, D. Wang, D. Zhang, L. Gao, T. Lin, Synergistic effects of carboxymethyl cellulose and ZnO as alkaline electrolyte additives for aluminium anodes with a view towards Al-air batteries, J. Power Sources 335 (2016) 1–11, https://doi.org/10.1016/j.jpowsour.2016.09.060.
[30] P. Tangthuam, J. Pimoei, A.A. Mohamad, F. Mahlendorf, A. Somwangthanaroj, S. Kheawhom, Carboxymethyl cellulose-based polyelectrolyte as cationic exchange membrane for zinc-iodine batteries, Heliyon 6 (2020) e05391, https://doi.org/10.1016/j.heliyon.2020.e05391.
[31] A. Abbasi, S. Hosseini, A. Somwangthanaroj, A.A. Mohamad, S. Kheawhom, Poly (2,6-dimethyl-1,4-phenylene oxide)-based hydroxide exchange separator membranes for zinc-air battery, Int. J. Mol. Sci. 20 (2019) 3678–3695, https://doi.org/10.3390/ijms20153678.
[32] M.T. Tsehaye, G. Teklay Gebreslassie, N. Heon Choi, D. Milian, V. Martin, P. Fischer, J. Tübke, N. El Kissi, M.L. Donten, F. Alloin, C. Iojoiu, Pristine and modified porous membranes for zinc slurry-air flow battery, Molecules 26 (2021) 4062–4082, https://doi.org/10.3390/molecules26134062.
[33] D. Stock, S. Dongmo, J. Janek, D. Schröder, Benchmarking anode concepts: the future of electrically rechargeable zinc-air batteries, ACS Energy Lett. 4 (2019) 1287–1300, https://doi.org/10.1021/acsenergylett.9b00510.
[34] B.S. Lee, S. Cui, X. Xing, H. Liu, X. Yue, V. Petrova, H.D. Lim, R. Chen, P. Liu, Dendrite suppression membranes for rechargeable zinc batteries, ACS Appl. Mater. Interfaces 10 (2018) 38928–38935, https://doi.org/10.1021/acsami.8b14022.
[35] A. Shen, Y. Zou, Q. Wang, R.A.W. Dryfe, X. Huang, S. Dou, L. Dai, S. Wang, Oxygen reduction reaction in a droplet on graphite: direct evidence that the edge is more active than the basal plane, Angew. Chem. Int. Ed. 53 (2014) 10804–10808, https://doi.org/10.1002/anie.201406695.
[36] D. Qu, Investigation of oxygen reduction on activated carbon electrodes in alkaline solution, Carbon 45 (2007) 1296–1301, https://doi.org/10.1016/j.carbon.2007.01.013. N Y.
[37] E. Yeager, Electrocatalysts for O_2 reduction, Electrochim. Acta 29 (1984) 1527–1537, https://doi.org/10.1016/0013-4686(84)85006-9.
[38] Y. Qi, S. Yuan, L. Cui, Z. Wang, X. He, W. Zhang, T. Asefa, (Fe,Co)/N-doped multi-walled carbon nanotubes as efficient bifunctional electrocatalysts for rechargeable zinc-air batteries, ChemCatChem 13 (2021) 1023–1033, https://doi.org/10.1002/cctc.202001131.
[39] N.K. Wagh, D.H. Kim, S.H. Kim, S.S. Shinde, J.H. Lee, Heuristic iron-cobalt-mediated robust pH-universal oxygen bifunctional lusters for reversible aqueous and flexible solid-state Zn-air cells, ACS Nano 15 (2021) 14683–14696, https://doi.org/10.1021/acsnano.1c04471.
[40] W. Sun, F. Wang, B. Zhang, M. Zhang, V. Küpers, X. Ji, C. Theile, P. Bieker, K. Xu, C. Wang, M. Winter, A rechargeable zinc-air battery based on zinc peroxide chemistry, Science 371 (2021) 46–51. https://www.science.org/doi/10.1126/science.abb9554.
[41] M.A. Al-Saleh, S. Gültekin, A.S. Al-Zakri, H. Celiker, Effect of carbon dioxide on the performance of Ni/PTFE and Ag/PTFE electrodes in an alkaline fuel cell, J. Appl. Electrochem. 24 (1994) 575–580, https://doi.org/10.1007/BF00249861.
[42] M.T. Tsehaye, F. Alloin, C. Iojoiu, R.A. Tufa, D. Aili, P. Fischer, S. Velizarov, Membranes for zinc-air batteries: recent progress, challenges and perspectives, J. Power Sources 475 (2020), 228689, https://doi.org/10.1016/j.jpowsour.2020.228689.
[43] D.C. Johnston, Stretched exponential relaxation arising from a continuous sum of exponential decays, Phys. Rev. B 74 (2006), 184430, https://doi.org/10.1103/PhysRevB.74.184430.